

Basic Science Model of Blood as an Electron-Delivery Circuit Describes the Evolution of the Human Circulation

William S. Peters*

University of Auckland, New Zealand

*Corresponding author: Peters WS, University of Auckland, New Zealand, Tel: +64 21 0815 3109; E-mail: wllmpters@gmail.com

Received Date: Jan 06, 2017; Accepted Date: Mar 19, 2017; Published Date: Apr 11, 2017

Copyright: © 2017 Peters WS. This is an open-access article distributed under the terms of the Creative Commons Attribution License, which permits unrestricted use, distribution, and reproduction in any medium, provided the original author and source are credited.

Abstract

A basic science model of the closed one-way circulation of redoxing haem in vertebrates is detailed. The adaptive, mechanistic model is of an electron-delivery circuit bounded by the geomagnetic field and electromagnetic radiation and it accounts for a quantum conformational change in circulatory topography from fish to human via a transitional reptilian circulation. The model is nested within a macro-evolutionary view of plants and animals as countervailing poles of a light-enabled redoxing biosphere. The model is reconciled with human embryogenesis and evolution. If proven broadly applicable, this basic science model will allow for a greater understanding of vertebrate embryogenesis and circulatory physiology.

The author acknowledges the support of Prof. John Windsor FRACS FRSNZ (Department of Surgery, University of Auckland, NZ), Mr F. Paget Milsom FRACS (Cardiothoracic Surgery, Auckland City Hospital, NZ) and Prof. Peter Hunter FRS and David Ladd PhD (Auckland Bioengineering Institute, University of Auckland, NZ). Thanks also to the Australasian Society of Cardiothoracic Surgeons for a research grant (2006) and to Don Campbell ME (Matrix Applied Computing, NZ) and Jeff Smith (Deep Animation, NZ).

Keywords: Vertebrate; Morphogenesis; Evolution; Blood; Circulation; Redox; Paramagnetic

Introduction

Within the redoxing biosphere, human life is structurally enveloped and retains stability of a 'native state' [1-7]. From the nature of reactive oxygen species produced by mitochondrial respiration to chromatin accessibility and gene regulation, hierarchical, spatio-temporal events tie redox activity to human embryogenesis and physiological function [8-12]. Hemodynamic forces and hypoxia also have measurable effects on embryogenesis [13].

The circulation of blood is fundamental to vertebrate life and the notion of the circulation as a closed, one-way circuit to deliver oxygen to the organism underpins human physiology [14].

Haem, a iron-based porphyrin of deep homology [15], has unique polar switching and light absorbing properties that are exploited in magnetic resonance imaging and light spectroscopy but are not accounted for in circulatory physiology.

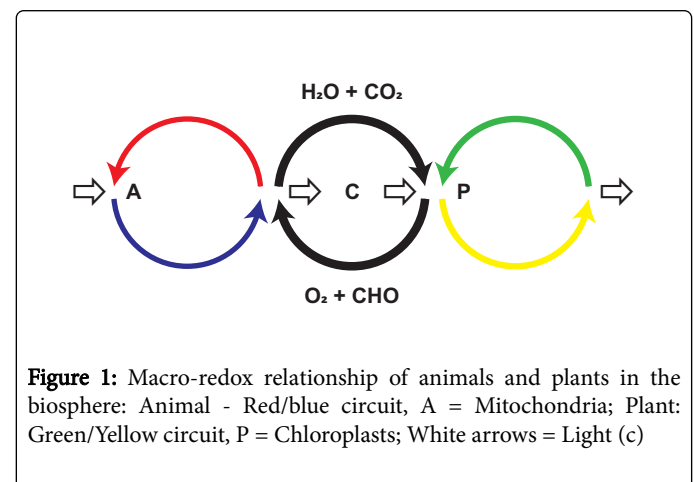
This manuscript examines the idea that the magnetic properties of circulating haem, which switch polarity with oxidation state, influence evolution of the circulatory system. A physical model of the circulation as an electron-delivery circuit, with oxygen consumed by mitochondria for cellular energy production and growth [16,17], is presented within the context of a countervailing, animal-plant redoxing biosphere.

Redoxing biosphere

Figure 1 shows the macro-redox relationship of animals and plants in the biosphere. Haem delivers oxygen to the animal. Mitochondria

consume oxygen and produce energy and water. Plants utilize a complimentary magnesium-based porphyrin, chlorophyll, found in chloroplasts, to consume water and produce energy and oxygen.

In this macro-redoxing framework, haem-based circuits carry electrons in the opposite direction to chlorophyll-based circuits. In contrast, the haem and chlorophyll circuits both create energy for structuring life-forms (Figure 1).



The flow of electrons through the multitudes of individual animal and plant circuits grounded in the biosphere follows a continuous, one-way path and a differential redox state between the two countervailing groups exists. A source of energy into animal and plant life-forms comes from electromagnetic radiation in the visible light range passing through the biosphere.

In animals, bio-photons [18] are pulled into haem in the peripheries as oxygen is released for consumption and then expelled centrally from haem as oxygen is bound. This contrasts with plants: photons enter chlorophyll in the leaves where water is consumed and biophotons are seen in the roots, where water is imbibed [19].

Basic Physics Relating to the Closed Circulation of Blood

Physical properties of haem electron-transfer circuits

In the representative vertebrate circuit of Figure 1, blood flow is one-way. Oxygen is bound in the pharyngeal-derived capillary bed; the gills or the lungs. On binding, the unpaired electrons of haem and oxygen are shared. Blood switches polarity from paramagnetic to diamagnetic [20,21]. After disassociating from oxygen in the systemic capillaries, circulating blood returns to its paramagnetic state, making for a 360° phase shift in the closed circuit.

The light absorption differential of redoxing haem peaks in the visible range and explains the change in colour of blood with oxygenation [22]. Deoxygenated, paramagnetic blood has a high affinity for light absorption and appears dark (blue). After binding oxygen, light is reflected by haem and diamagnetic blood appears bright (red).

As is true for plants, light is a part of the animal equation.

Single and double-looped circuits of fish and humans, respectively

In fish, blood passes through the heart only once in completing a full circuit of the body [23]. De-oxygenated blood is ejected from the heart to the gills. Oxygenated gill blood then passes via the dorsal aorta to the body before returning to the heart de-oxygenated.

The fish circulation is represented using a tube to describe the closed, one-way passage of blood (Figure 2a). A single 360° axial rotation, left or right, in a length of tubing is required to create the cardiac loop and configure the closed circuit. The central blue loop represents the midline, single ventricle heart common to fish.

In humans, the closed blood pathway makes two loops through the heart to complete one circuit of the body (Figure 2d) [24]. Blood passes from the body via the right heart, then through a pulmonary passage where it is oxygenated [14], before it loops back through the left heart and out behind the pulmonary outlet via the aorta to the body to complete the circuit. The central blue and red loops represent the right and left atrio-ventricular loops of the heart, respectively, with the pulmonary passage positioned between.

To configure the basic human circuit requires both left and right (or right and left) 360° axial, or longitudinal twists in the tube.

In both fish and humans, the polar-switching closed circuits operating in the geomagnetic field have a net zero-degree phase-shift, yet the human circuit contains an extra 360°, anti-axially rotated loop not accounted for by the serial phase-shifts of circulating, redoxing haem. Also, the human circuit is vertically disposed relative to gravity, compared to the horizontally disposed fish circuit.

Mechanism of transformation

In the basic circulatory model of the fish, the in-series pharyngeal (gill) and systemic (body) capillary beds are shown as isolated from one another (Figure 2a). This inert system is used as a starting point for understanding the mechanism of translation to a double-looped human circuit.

Where the blue inflow crosses the red outflow centrally, a slip of diamagnetic blood is caught into the central paramagnetic stream. The shunt breaks the hermetic state of the in-series polar-switched circulatory system (Figure 2b). This slipstream turns away from its repellent host as it runs with the paramagnetic stream through the heart. Rotating anti-axially 360°, the spiralled thread exits the heart, winding behind the stream of the truncus arteriosus and into upper gill arches to reach the dorsal aorta to complete a 'loop-in-loop' trajectory.

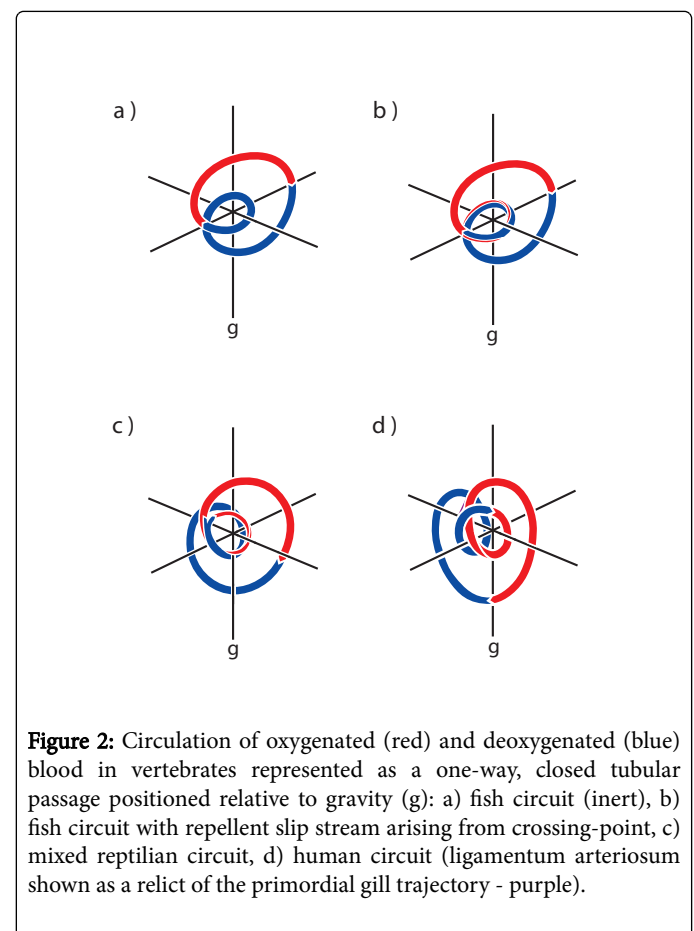


Figure 2: Circulation of oxygenated (red) and deoxygenated (blue) blood in vertebrates represented as a one-way, closed tubular passage positioned relative to gravity (g): a) fish circuit (inert), b) fish circuit with repellent slip stream arising from crossing-point, c) mixed reptilian circuit, d) human circuit (ligamentum arteriosum shown as a relict of the primordial gill trajectory - purple).

Across nature, symmetry-breaking action is typically left-handed [25-27].

The nascent repellent loop-in-loop arrangement pivots apart (Figure 2c). Oxygen tension shifts across the pharyngeal capillary network and gill filaments snap through into permissive space, involuting to become alveoli. De-oxygenated blood splits from the primary cardiac outflow and pursues the morphing pharyngeal bed. A pulmonary pathway establishes.

The remainder of the de-oxygenated stream continues to perfuse the devolving gill-capillary network. This remnant primary gill trajectory is the ductus arteriosus.

As the loop-in-loop strengthens, the one-way, mixed circuit rotates about a central axis perpendicular to gravity. This staging of loop-in-loop progression represents the mixed reptilian circulation [28-30]. Flows between the split loops calibrate accordingly [31].

Modeling Evolution of the Human Circulation

Anatomy of the fish circulation

The one-way single-looped fish circuit is represented anatomically in Figure 3 and is used as the starting point for modelling evolution of the human circulation.

Anatomically, blood flows counter-current. Oxygenated blood radiates cephalad and caudal from the dorsal aorta to the somitomer segments that make up the body and deoxygenated blood returns via the cardinal veins (Figure 3).

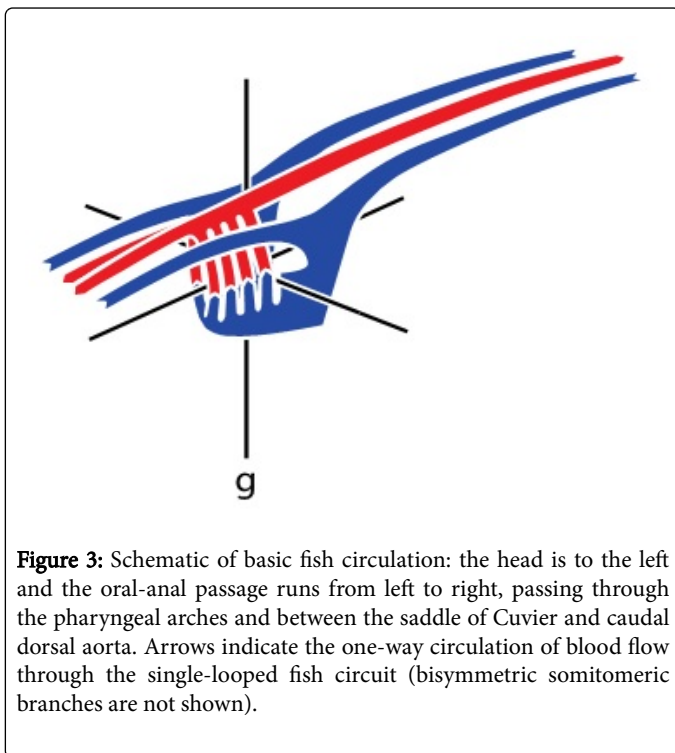


Figure 3: Schematic of basic fish circulation: the head is to the left and the oral-anal passage runs from left to right, passing through the pharyngeal arches and between the saddle of Cuvier and caudal dorsal aorta. Arrows indicate the one-way circulation of blood flow through the single-looped fish circuit (bisymmetric somitomer branches are not shown).

Dorsal aortic blood is distributed via bisymmetric somitomer arteries to the body walls [32]. Oxygen dissociates at each corpuscle's apogee in a co-operative and co-ordinated hair-pin fold relative the orthogonal plane and light is drawn in.

Deoxygenated blood returns via the four cardinal veins and bilateral Ducts of Cuvier to the venous pole of the midline heart. Paramagnetic streams coalesce centrally. Aliquots repeatedly damp in the midline ventricle and eject at a reverse 45° angle from the heart out the arterial pole. Blood passes through paired pharyngeal gill arches and is oxygenated. Light is released.

The single-looped circuit has a bisymmetric, centipedal-like somitomer perfusion pattern about the oral-anal sagittal plane. The

body walls meet in the midline ventrally and enclose the oral-anal passage. No named vessels cross this fibrous divide.

Relative the geomagnetic field, a homeostatic center of redox and magnetic moment is maintained by the standing-wave topology of the polar-switched circulation. Courtesy of the counter-current flow of redoxing blood, a one-way, co-moment compulsion about a central axis perpendicular to gravity may provide a gyroscopic stability to the horizontally-disposed fish circuit.

Cardiogenesis, pharyngeal arches and somitomer perfusion

In human embryogenesis, the heart appears at first like the fish's: a midline tube with venous and arterial poles.

Starting conceptually with the inert fish circulation, a slip of allantoic diamagnetic blood is caught into the confluence of paramagnetic streams at the venous pole and sets up the loop-in-loop circuit (Figure 4a). The repellent slip rotates anti-axially as it streams with the primary atrio-ventricular loop into and out of the heart. An atrial septal, salamander sliver forms in the void between the disparate streams [28]. In humans, the non-valved left atrial funnel appears out of no precursor structures [33].

The ventral poles of the repellent loop-in-loop arrangement pivot apart (Figure 4b). The diamagnetic bloodstream trajectory cantilevers via third and fourth gill arches to the dorsal aorta [34]. The primary paramagnetic trajectory cantilevers opposite, tilting into the sixth arch branches. The flow of paramagnetic blood splits to pursue the involuting pharyngeal bed and the pulmonary pathway establishes. The fifth arches, a magnetic no-mans-land, desiccate [35].

In the heart, the co-current, counter-moment loop-in-loop trajectories stream separately in the single ventricle [30]. A reptilian ventricular ridge develops in the magnetic void between the divergent ventral loops. The functional separation of the two streams through the single ventricle allows blood to be variably distributed to the upper body and arch via the truncus arteriosus, the distal body via the ductus arteriosus and through the interposed pulmonary circulation via the pulmonary trunk.

With strengthening of the co-current, counter-moment ventral loop-in-loop, the circuit precesses. As spiralled truncus arteriosus flow replaces bi-linear dorsal aortic perfusion, distribution to the somitomer segments morphs in orderly choreography toward a pentameric patternation. Bisymmetry is retained about the oral-anal sagittal plane. The head comes up and the thorax broadens, fins become limbs [36,37] and post-coccygeal tail segments foreshorten.

Closure of the ductus arteriosus and progression to bipedalism

As the central loops equilibrate and move toward a perpendicular parity, loop-in-loop septation completes in the spiraled void between (Figure 4c) [38].

With separation from the allantoic supply, blood circuit topography is set. In mammals, birds and humans, topological re-organisation of the one-way circulation of blood has progressed to the point that the oxygen-sensitive ductus arteriosus closes at birth. All bodily blood is now physically directed via the pulmonary nest [39] and the double-looped circuit is complete. A small (one percent) residual bronchial shunt persists in the human double-looped circuit.

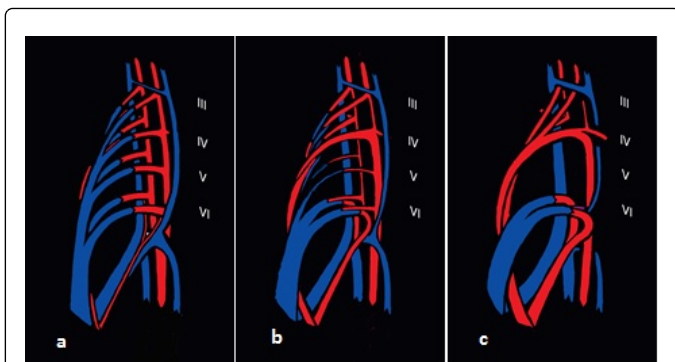


Figure 4: Representation of the heart and pharyngeal arches in vertebrates as blood flow trajectories (arches are classically identified as III-VI, on left): a) fish circuit with repellent slip stream arising from crossing-point (allantoic entry – white dot), b) mixed reptilian circuit, c) human circuit (ligamentum arteriosus shown as a relict of the primordial gill trajectory – purple line).

The pulmonary trunk and aortic arch of humans and birds are splayed wider apart compared to quadruped mammals. In the human heart, the two loops are set near-ninety degrees apart (Figure 5). Transition of the loop-in-loop circuit toward perpendicular parity is coupled with circuit precession and this is seen further advanced in bipedal birds and humans.

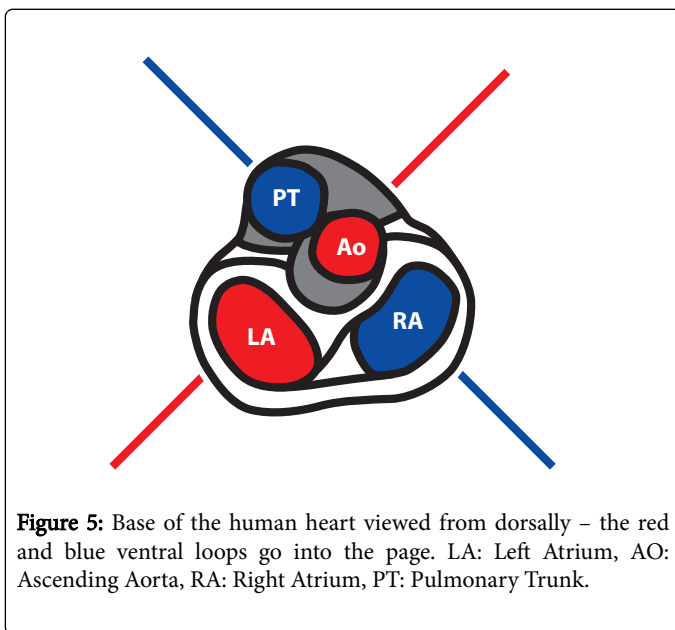


Figure 5: Base of the human heart viewed from dorsally – the red and blue ventral loops go into the page. LA: Left Atrium, AO: Ascending Aorta, RA: Right Atrium, PT: Pulmonary Trunk.

Geometric expression

The geometric translational description of the transitional loop-in-loop circuit is caught in the pivoting panes of a centrally rotated flat-pack frame (Figure 6). The hinge represents the sagittal midline. The frame pivots apart and precesses about its center, degree for degree, from greater than zero degrees to less than ninety degrees (zero and ninety degrees represent inert, non-transitional states).

Bisymmetry is maintained through the hinge-line. A hysteretic sigmoidal shaping may be reflected in the precessed human spine.

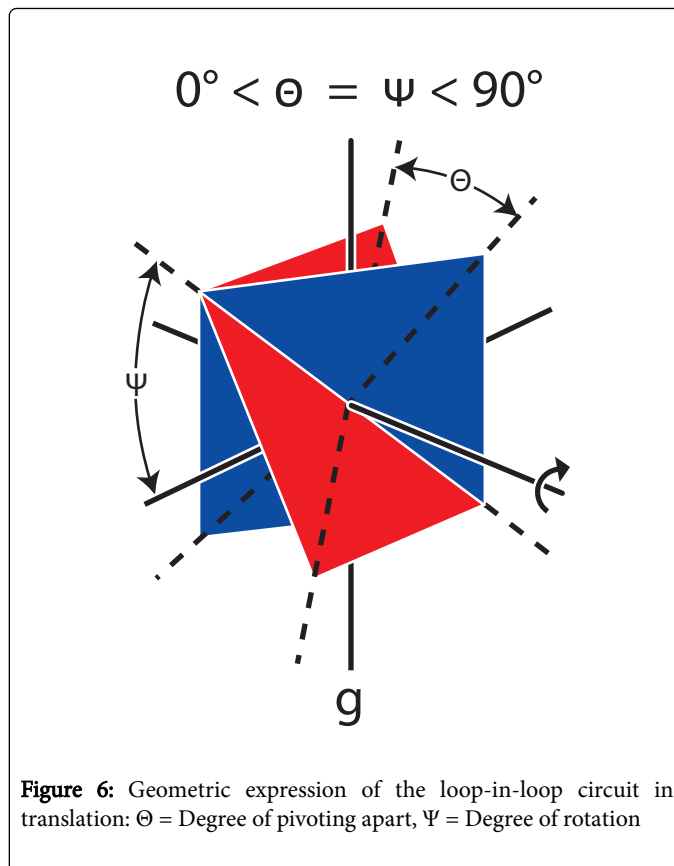


Figure 6: Geometric expression of the loop-in-loop circuit in translation: Θ = Degree of pivoting apart, Ψ = Degree of rotation

In the clinical condition of dextrocardia, the heart and great vessels are in a mirrored position internally but the person's outward morphology remains the same [40]. In dextrocardia the symmetry-breaking diamagnetic slip initiates a right-hand versus a left-hand spiralled path about the paramagnetic primary loop. Biymmetric somitomer perfusion is maintained by a pentagraphic re-distribution.

As in nature, in classical geometry left and right-handed logarithmic spirals find bisymmetry in a pentagram [41,42]. The physical model, as predicated by the left-right or right-left double-looped human tubular circuit, is chiral.

Further interrogation of embryological and anatomical conformations with respect to the mechanistic model are described elsewhere [43].

Ambient oxygen and the adaptive circulation model

In the closed circulation of blood in vertebrates, the oxygen ingress and egress capillary beds lay in series between counter-current paramagnetic and diamagnetic passageways. *In vivo*, the pharyngeal bed sits within the systemic bed, providing a zone of overlap.

Anatomically, this overlap exists in the region of the pharyngeal arches and the confluence of the cardinal veins. The anterior jugular vein that drains the lower pharynx in some fish is an example of this phenomenon [23].

Separate from the allantoic supply, this zone of overlap creates an opportunity in the individual for quantiles of oxygenated blood to

bypass the passage to the body and add to (or subtract from) the loop-in-loop transistor state. Circuit topography adjusts accordingly.

Physically, the least mixed circuitry is represented in fish and bipeds. In the geometric expression of circulatory evolution, the loop-in-loop circuitries nominally sit in the one to 15° and 75-89° ranges of the quantum-shifted translational model, respectively. The loop-in-loop transistor in the salamander/reptilian phase may be thought of nominally as laying somewhere between 25-65°.

The pendulous nature of the oxygen-driven, quantum-shifted circulation model suggests that animals such as salamanders have a more transitional, but less efficient, circuitry. Ambient oxygen levels influence growth in animals with a mixed circulation such as mudskippers and alligators [44,45]. The rete mirabile, a prominent feature in some fish and reptiles, may allow greater circulatory redox variance and hysteresis by acting as a counter-current sink [46].

Conclusion

The mechanistic model describes the evolution of the human circulation from fish, through the physics of the closed circulation of redoxing haem. The model tracks embryological, anatomical and evolutionary form, from fish to man, and is nested within a macro-redoxing biosphere.

The model is chiral and shows the remnant ductus arteriosus in humans, the ligamentum arteriosum, as a relict of the simpler, primordial closed circulation. The predictive model aligns with the notion of accommodation [47] but physically bounds evolution of form [48].

The model does not consider the origin of pulsatility in the blood circuit and it excludes other macro-redoxing activities in the biosphere.

In embryogenesis and adult life, cell fate decision and maintenance is controlled by transcription factors and other redox signaling cues acting on the genome [49]. The role of the topologically-organised, redoxing haem circuit in vertebrate mitochondrial energy production and body-wide cellular expression deserves further investigation.

References

1. Falkowski PG, Godfrey LV (2008) Electrons, life and the evolution of Earth's oxygen cycle. *Philos Trans R Soc Lond B Biol Sci* 363: 2705-2716.
2. Reinhard CT, Planavsky N, Olson S, Lyons TW, Erwin DH (2016) Earth's oxygen cycle and the evolution of animal life. *Proc Natl Acad Sci USA* 113: 8933-8932.
3. Jelen B, Giovannelli D, Falkowski P (2016) The role of microbial electron transfer in the coevolution of the biosphere and geosphere. *Annu Rev Microbiol* 70: 45-62.
4. Duboc V, Lepage T (2006) A conserved role for nodal signalling pathway in the establishment of dorso-ventral and left-right axes in deuterostomes. *Exp Zool B, Mol Dev E* 310B: 41-53.
5. Shubin N, Tabin C, Carroll S (2009) Deep homology and the origins of evolutionary novelty. *Nature* 457: 818-823.
6. Laland KN, Uller T, Feldman MW, Sterelny K, Müller GB, et al. (2015) The extended evolutionary synthesis: Its structure, assumptions and predictions. *Proc Biol Sci*. 282:20151019.
7. Bastolla U, Dehouck Y, Echave J (2016) What evolution tells us about protein physics, and protein physics tells us about evolution. *Curr Opin Struct Biol* 42: 59-66.
8. Brand MD (2016) Mitochondrial generation of superoxide and hydrogen peroxide as the source of mitochondrial redox signaling. *Free Radic Biol Med* 100: 14-31.
9. Angelova PR, Abramov AY (2016) Functional role of mitochondrial reactive oxygen species in physiology. *Free Radic Biol Med* 100: 81-85.
10. Gut P, Verdin E (2013) The nexus of chromatin regulation and intermediary metabolism. *Nature* 502: 489-498.
11. Fraser J, Ferrai C, Chiariello AM, Schueler M, Rito T, et al. (2015) Hierarchical folding and reorganization of chromosomes are linked to transcriptional changes in cellular differentiation. *Mol Syst Biol* 11: 852.
12. Weber B, Zicola J, Oka R, Stam M (2016) Plant enhancers: A call for discovery. *Trends Plant Sci* 21: 974-987.
13. Culver JC, Dickinson ME (2010) The effects of hemodynamic force on embryonic development. *Microcirculation* 17: 164-178.
14. Azizi MH, Nayernouri T, Azizi F (2008) A brief history of the discovery of the circulation of blood in the human body. *Arch Iran Med* 11: 345-350.
15. Hardison R (1998) Hemoglobin from bacteria to man: Evolution of different patterns of gene expression. *J Exp Biol* 201: 1099-1117.
16. Bianconi E, Piovesan A, Facchin F, Beraudi A, Casadei R, et al. (2013) An estimation of the number of cells in the human body. *Ann Hum Biol* 40: 463-471.
17. Wisnovsky S, Lei EK, Jean SR, Kelley SO (2016) Mitochondrial chemical biology: New probes elucidate the secrets of the powerhouse of the cell. *Cell Chem Biol* 23: 917-927.
18. Nair R, Maseeh A (2012) Vitamin D: The "sunshine" vitamin. *J Pharmacol Pharmacother* 3: 118-126.
19. Lee HJ, Ha JH, Kim SG, Choi HK, Kim ZH, et al. (2016) Stem-piped light activates phytochrome B to trigger light responses in *Arabidopsis thaliana* roots. *Sci Signal* 9: 106.
20. Okazaki M, Maeda N, Shiga T (1987) Effects of an inhomogeneous magnetic field on flowing erythrocytes. *Eur Biophys J* 14: 139-145.
21. Formicki K, Winnicki A (1998) Reactions of fish embryos and larvae to constant magnetic fields. *Italian Journal of Zoology* 65: 479-482.
22. Nordlund TM (2011) Quantitative understanding of biosystems: An introduction to biophysics. CRC Press Textbook 588; 320.
23. Graham JB (1997) Air-breathing fishes: Evolution, diversity, and adaptation. Academic Press.
24. Harvey W (1628) *De Motu Cordis*. Frankfurt: Sumptibus Guilielmi Fitzeri.
25. Bischoff M, Parfitt DE, Zernicka-Goetz M (2008) Formation of the embryonic-abembryonic axis of the mouse blastocyst: relationships between orientation of early cleavage divisions and pattern of symmetric/asymmetric divisions. *Development* 135: 953-962.
26. Davison A, McDowell GS, Holden JM, Johnson HF, Koutsovoulos GD, et al. (2015) Formin is associated with left-right asymmetry in the pond snail and the frog. *Curr Biol* 26: 654-660.
27. Novotny M, Kleywegt GJ (2005) A survey of left-handed helices in protein structures. *J Mol Biol* 347: 231-241.
28. Francis ETB (1934) *The anatomy of the salamander*. Oxford, The Clarendon Press, UK.
29. Wyneken J (2009) Normal reptile heart morphology and function. *Vet Clin North Am Exot Anim Pract* 12: 51-63.
30. Hicks JW (2002) The physiological and evolutionary significance of cardiovascular shunting patterns in reptiles. *News Physiol Sci* 17: 241-245.
31. Condos WR Jr, Latham RD, Hoadley SD, Pasipoularides A (1987) Hemodynamics of the Mueller maneuver in man: right and left heart micromanometry and Doppler echocardiography. *Circulation* 76: 1020-1028.
32. Jacobson AG (1988) Somitomeres: Mesodermal segments of vertebrate embryos. *Development* 104: 209-220.
33. Anderson RH, Brown NA, Moorman AF (2006) Development and structures of the venous pole of the heart. *Dev Dyn* 235: 2-9.
34. Morbiducci U, Ponzini R, Rizzo G, Cadioli M, Esposito A, et al. (2009) In vivo quantification of helical blood flow in human aorta by time-resolved three-dimensional cine phase contrast magnetic resonance imaging. *Ann Biomed Eng* 37: 516-531.

35. Gupta SK, Bamforth SD, Anderson RH (2015) How frequent is the fifth arch artery? *Cardiol Young* 25: 628-646.
36. Adachi N, Robinson M, Goolsbee A, Shubin NH (2016) Regulatory evolution of *Tbx5* and the origin of paired appendages. *Proc Natl Acad Sci USA* 113: 10115-10120.
37. Sanger TJ, Revell LJ, Gibson-Brown JJ, Losos JB (2012) Repeated modification of early limb morphogenesis programmes underlies the convergence of relative limb length in *Anolis* lizards. *Proc Biol Sci* 279: 739-748.
38. Laane HM (1979) The septation of the arterial pole of the heart in the chick embryo. III. Development of the truncus arteriosus of the heart of chick embryos from 5 1/2 to 7 days of incubation. *Acta Morphol Neerl Scand* 17: 1-20.
39. Schneider DJ, Moore JW (2006) Patent Ductus Arteriosus. *Circulation* 114: 1873-1882.
40. Chen CM, Norris D, Bhattacharya S (2010) Transcriptional control of left-right patterning in cardiac development. *Pediatr Cardiol* 31: 371-377.
41. Ghyka M (1977) *The Geometry of Art and Life*. Dover Publications, New York.
42. Bredder CM (1955) Observations on the occurrence and attributes of pentagonal symmetry. *Bulletin of the American Museum of Natural History* 106: 3.
43. Peters WS (2015) *Per Sanguinem Nostrum*. Auckland, NZ: William Peters.
44. Jew CJ, Wegner NC, Yanagitsuru Y, Tresguerres M, Graham JB (2013) Atmospheric oxygen levels affect mudskipper terrestrial performance: implications for early tetrapods. *Integr Comp Biol* 53: 248-257.
45. Owerkowicz T, Elsey RM, Hicks JW (2009) Atmospheric oxygen level affects growth trajectory, cardiopulmonary allometry and metabolic rate in the American alligator (*Alligator mississippiensis*). *J Exp Biol* 212: 1237-1247.
46. Porter WR, Witmer LM (2015) Vascular Patterns in Iguanas and Other Squamates: Blood Vessels and Sites of Thermal Exchange. *PLoS One* 10: e0139215.
47. Darwin C (1859) *On the origin of species by means of natural selection*. John Murray, London.
48. Vitruvius-Pollio M (2009) *Vitruvius De Architectura*.
49. Festuccia N, Gonzalez I, Navarro P (2016) The epigenetic paradox of pluripotent ES cells. *J Mol Biol* S0022-2836: 30538-1.